Defined spatiotemporal features of RAS-ERK signals dictate cell fate in MCF-7 mammary epithelial cells

Ana Herrero[†], Berta Casar, Paula Colón-Bolea, Lorena Agudo-Ibáñez, and Piero Crespo*
Instituto de Biomedicina y Biotecnología de Cantabria (IBBTEC), Consejo Superior de Investigaciones Científicas (CSIC), Universidad de Cantabria, Santander E-39011, Spain

ABSTRACT Signals conveyed through the RAS-ERK pathway are essential for the determination of cell fate. It is well established that signal variability is achieved in the different microenvironments in which signals unfold. It is also known that signal duration is critical for decisions concerning cell commitment. However, it is unclear how RAS-ERK signals integrate time and space in order to elicit a given biological response. To investigate this, we used MCF-7 cells, in which EGF-induced transient ERK activation triggers proliferation, whereas sustained ERK activation in response to heregulin leads to adipocytic differentiation. We found that both proliferative and differentiating signals emanate exclusively from plasma membrane–disordered microdomains. Of interest, the EGF signal can be transformed into a differentiating stimulus by HRAS overexpression, which prolongs ERK activation, but only if HRAS localizes at disordered membrane. On the other hand, HRAS signals emanating from the Golgi complex induce apoptosis and can prevent heregulin-induced differentiation. Our results indicate that within the same cellular context, RAS can exert different, even antagonistic, effects, depending on its sublocalization. Thus cell destiny is defined by the ability of a stimulus to activate RAS at the appropriate sublocalization for an adequate period while avoiding switching on opposing RAS signals.

INTRODUCTION

Signals conveyed through the RAS–extracellular signal-regulated kinase (ERK) axis (RAS-RAF–mitogen-activated protein kinase kinase [MEK]–ERK) play critical roles in multiple cellular functions, including cell fate decisions at the proliferation/differentiation/apoptosis crossroads. A large body of data shows that the RAS-ERK pathway operates in the determination of cell destiny by mechanisms that extend beyond its simple on–off status and that subtle variations in

several signal parameters can evoke profound alterations in its biological output (Kholodenko et al., 2010). For example, in mammary epithelial cells, the decision to proliferate depends on ERK's signal amplitude and frequency (Albeck et al., 2013). Signal duration is also critical in the determination of cell commitment. This was initially demonstrated in rat pheochromocytoma PC-12 cells, in which transient ERK activation, stimulated by epidermal growth factor (EGF), resulted in proliferation, whereas sustained ERK activation, evoked by nerve growth factor (NGF), induced cell differentiation (Traverse et al., 1992). This phenomenon has been observed in multiple cellular models, such as squamous cell lung carcinoma SCC-12F cells (McCawley et al., 1999) and Madin–Darby canine kidney epithelial cells, in which transient ERK activation resulting from EGF treatment induced proliferation, whereas prolonged ERK activation triggered by HGF led to the acquisition of mesenchymal features, including scattering (Liang and Chen, 2001).

In addition, a wealth of data has led to the abandonment of the view that the RAS-ERK pathway is a unique, linear signaling axis. It is now established that space plays a critical role in the RAS-ERK pathway by providing variability to its signals, depending on the availability of regulatory and effector molecules at the different

FIGURE 1: ERK activation kinetics induced by HRG and EGF in MCF-7 cells. (A) HRG-induced differentiation is dependent on ERK activation. Cells were treated with HRG (30 ng/ml) in the presence or absence of U0126 (10 μm) for 7 d before fixing and staining with Oil Red O. (B) Time course of ERK phosphorylation induced by treatment with EGF (50 ng/ml) or HRG (30 ng/ml) for the indicated times. Graphs are quantifications of the results obtained in three independent experiments (mean ± SEM). (C) Comparison of the intensity of ERK phosphorylation in response to EGF and HRG. Bar chart shows mean ± SEM of three independent experiments. *$p < 0.05$, **$p < 0.01$, ***$p < 0.001$ with 95% confidence interval.

tion that exhibits similar kinetics at the nucleus and the cytoplasm. Similarly, disordered membrane platforms are competent for inducing apoptosis. We show that over-expression of HRAS and other constituents of the RAS-ERK pathway leads to the prolongation of EGF-induced ERK activation and that this is sufficient to transform the EGF signal into a differentiating stimulus. Of interest, EGF evokes differentiation only if the overexpressed RAS localizes at disordered membrane microdomains but not at other sublocalizations. However, from the Golgi complex, RAS can induce apoptosis and antagonize differentiation signals. Our results demonstrate that specific spatial and temporal cues are critical for biological output determination as mediated by RAS-ERK signaling.
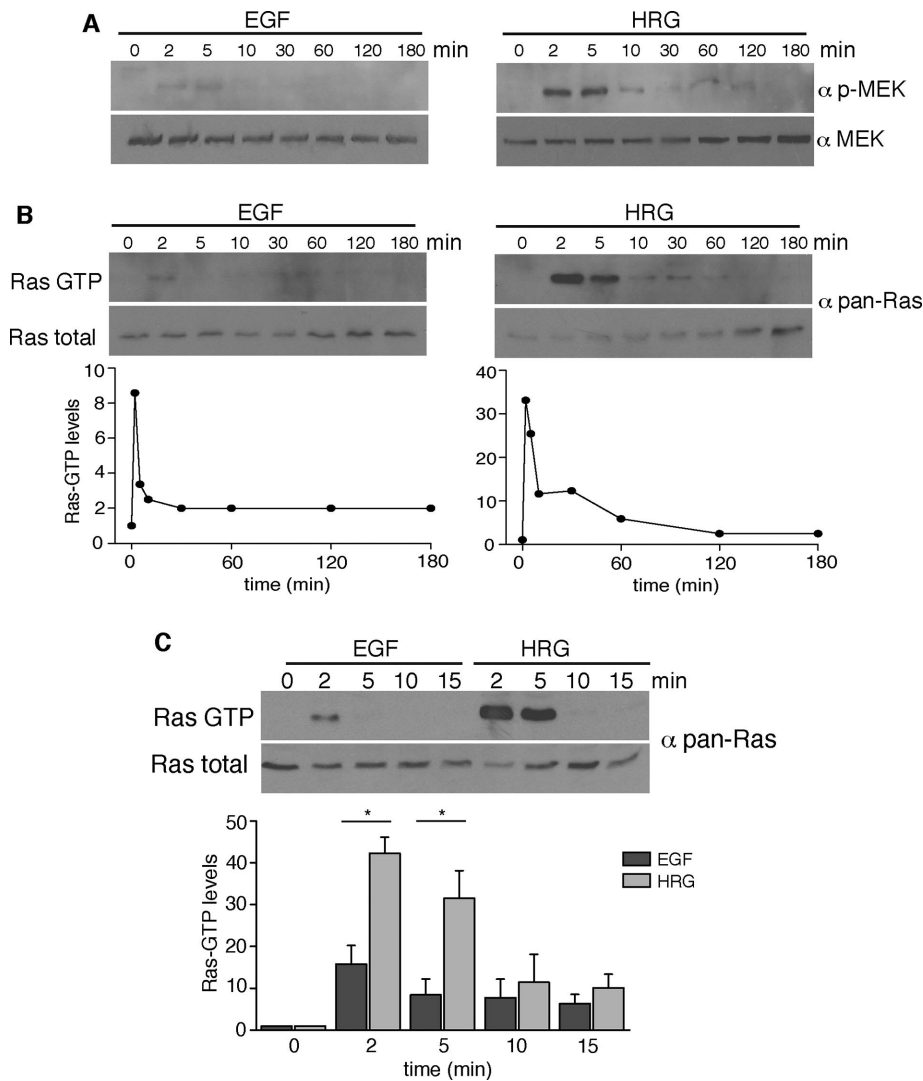
RESULTS

EGF and HRG evoke different activation kinetics for RAS-ERK pathway constituents

To study the spatiotemporal specificity of RAS-ERK signals associated with a given biological response, we used MCF-7 cells. This mammary epithelial cell line undergoes divergent fates, depending on the agonist acting on the EGF receptor family. EGF induces proliferation, whereas HRG evokes adipocytic-like differentiation (Nagashima et al., 2007), a process characterized by the accumulation of cytoplasmic lipid droplets, discernible by Oil Red staining. This phenomenon was entirely dependent on ERK activation, since treatment with the MEK inhibitor UO126 prevented differentiation completely (Figure 1A). Stimulation with HRG evoked sustained ERK activation for >1 h. In contrast, treatment with EGF resulted in an acute peak of ERK activity, lasting for barely 10 min (Figure 1B). At its peak levels, the intensity of ERK activation evoked by HRG was ~40% stronger than that induced by EGF treatment (Figure 1C).

We also monitored the activation of other upstream components of the RAS-ERK pathway in response to EGF/HRG treatment. HRG-induced MEK activation kinetics was only slightly prolonged in comparison to that resulting from EGF treatment (Figure 2A). This was also the case for RAS activation (Figure 2B), whereas HRG activated RAS more intensively than EGF (Figure 2C). Of interest, in response to HRG, MEK and RAS activation extended for a significantly shorter period than ERK phosphorylation (5 min vs. 1 h). These results demonstrated that the duration of ERK signal in response to HRG stimulation was primarily regulated at the level of ERK activation.

With respect to the activation pattern of ERK downstream effectors, we evaluated the activation of the cytoplasmic kinase RSK1 and the nuclear transcription factor ELK1. The activity of both substrates responded similarly: transiently to EGF and with sustained

microlocalizations from which RAS signals emanate, thereby regulating its biochemical and biological outputs in a site-specific manner (Calvo et al., 2010; Arozarena et al., 2011). However, it is unclear how RAS-ERK signals integrate time and space in order to elicit a given biological response.

To address this question, we used MCF-7 mammary epithelial cells, in which EGF-induced transient ERK activation triggers proliferation, whereas sustained ERK activation in response to treatment with heregulin (HRG) leads to adipocytic-like differentiation (Giani et al., 1998; Nagashima et al., 2007). We found that both EGF- and HRG-stimulated RAS signals emanate exclusively from disordered microdomains at the plasma membrane (PM), triggering ERK activa-

FIGURE 2: Activation kinetics for components of the RAS-ERK pathway induced by HRG and EGF. (A) Time course of MEK phosphorylation induced by treatment with EGF (50 ng/ml) or HRG (30 ng/ml) for the indicated times. (B) Time course of RAS GTP loading. Graphs are quantifications of the results obtained in three independent experiments (mean ± SEM). (C) Comparison of intensity of RAS GTP loading in response to EGF and HRG. Bar chart shows mean ± SEM of three independent experiments. *$p < 0.05$ with 95% confidence interval.

kinetics to HRG stimulation (Figure 3B). To elucidate whether ERK activation kinetics diverged at different subcellular compartments, we obtained nuclear and cytoplasmic extracts. Upon comparing the intensity of ERK activation at these sublocalizations, we found that both EGF and HRG stimulated stronger ERK activation at the cytoplasm than at the nucleus (Figure 3C). These results demonstrated that proliferative and differentiating stimuli evoked different activation kinetics for the different constituents of the RAS-ERK pathway.

## EGF and HRG activate RAS at defined sublocalizations

We sought to elucidate the membrane platforms from which RAS signals originated in response to agonist stimulation. To this end, we initially identified the types of membranes in which RAS was present in MCF-7 cells. Separation of endomembranes from plasma membrane fractions in sucrose gradients revealed that RAS was present in both types of structures (Figure 4A). We analyzed the PM sublocalization in further detail by separating detergent-resistant, lipid rafts, microdomains from soluble, disordered membrane (DM)

microdomains. We found that RAS, irrespective of which isoform, was exclusively present at DM locations and absent from lipid raft microdomains (Figure 4B).

Next we proceeded to assay how EGF and HRG activated RAS at those sublocalizations where it had been detected. As site-specific probes, we used HRAS wild-type constructs precisely sent to the desired sublocalization by fused sublocalization-specific tethers, namely PTP-HRAS, targeted to the endoplasmic reticulum (ER; Lorentzen et al., 2010); KDELr-HRAS, tethered to the Golgi complex (GC); and CD8-HRAS, sent to DM sublocalizations (Arozarena et al., 2004; Matallanas et al., 2006). We found that neither EGF nor HRG induced activation of RAS at the ER, whereas the PTP-HRAS probe was responsive to overexpression of RASGRF1, the exchange factor responsible for activating RAS at the ER (Arozarena et al., 2004; Figure 4C). A similar situation was observed for the KDELr-HRAS GC probe, which underwent GDP/GTP (guanidine biphosphate/guanidine triphosphate) exchange in the presence of overexpressed RASGRP1 (Caloca et al., 2003) but not when stimulated by EGF or HRG (Figure 4D). Conversely, CD8-HRAS, monitoring RAS activation at DM, underwent nucleotide exchange when cells were stimulated either by EGF or HRG (Figure 4E), with kinetics resembling those previously detected for endogenous RAS (Figure 2B).

In parallel, we performed live-cell RAS activation analyses using as a probe for RAS-GTP E3-R3 (A/D) a chimeric protein made of the RAF Ras-binding domain (RBD) fused to three enhanced green fluorescent proteins (GFPs) in tandem (Augsten et al., 2006). This construct was cotransfected together with cherry HRAS into MCF-7 cells, which were subsequently challenged by EGF and HRG treatments. We found that upon EGF stimulation, RAS activation was restricted to the cellular periphery, in full agreement with previous results (Song et al., 2013). Similarly, treatment with HGR resulted in pronounced recruitment of the probe to the PM but not to internal structures (Figure 5). These data suggested that both proliferative and differentiating signals required RAS activation at the PM but not at endomembranes.

To substantiate these findings further, we tested how specifically blocking RAS activation at the sublocalizations under scrutiny affected proliferation and differentiation. We used HRAS N17 dominant inhibitory versions targeted to the aforementioned sublocalizations, previously demonstrated to specifically inhibit RAS activation there (Matallanas et al., 2006). It was found that whereas DM-targeted CD8-HRAS N17 markedly inhibited HRG-induced differentiation, this was unaffected by the expression of the GC- and ER-tethered HRAS inhibitory mutants (Figure 6A). A similar situation was observed when we evaluated cellular proliferation (Figure 6B). Overall these results demonstrated that in MCF-7 cells, both proliferative and differentiating RAS-ERK signals emanate from the same sublocalization: the disordered membrane microdomains.
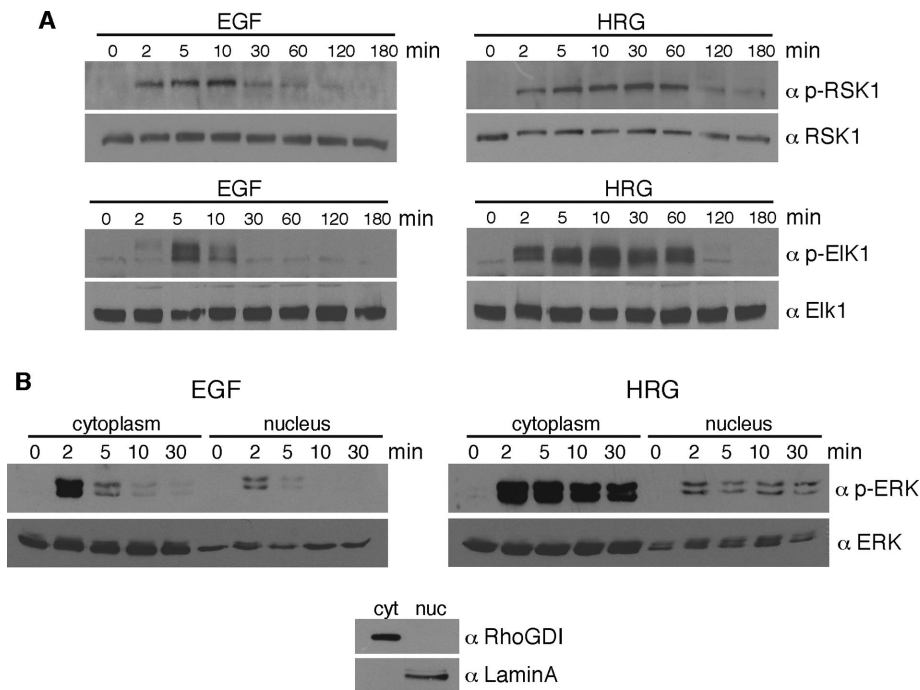
FIGURE 3: Activation kinetics of ERK cytoplasmic and nuclear effectors induced by HRG and EGF. (A) Time course of RSK1 and ELK1 phosphorylation induced by treatment with EGF (50 ng/ml) or HRG (30 ng/ml) for the indicated times. (B) Time course of ERK phosphorylation in nuclear and cytoplasmic fractions of cells stimulated with EGF or HRG for the indicated times. The purity of the fractions was ascertained by immunoblotting with lamin A and RhoGDI as nuclear and cytoplasmic markers, respectively.
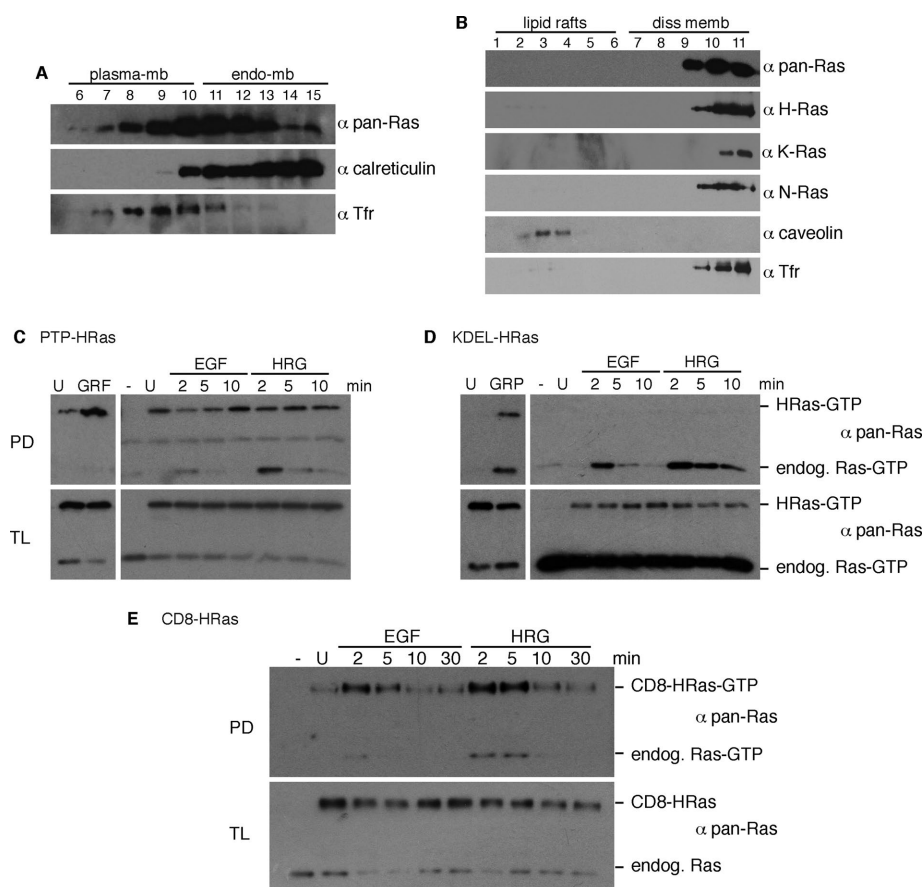

Overexpression of HRAS transforms EGF signal into a differentiation stimulus

The foregoing results indicated that signal kinetics rather than signal localization marked the difference between RAS-ERK–induced proliferative and differentiating outputs. Thus we tested whether by altering signal duration we could transform the EGF-induced proliferative signal into a stimulus evoking differentiation. For this purpose, we overexpressed several members of the RAS-ERK pathway in MCF-7 cells. This resulted in significant prolongation of ERK activation in response to EGF treatment (Figure 7, A and B). Whereas EGF was incapable of inducing differentiation by itself, EGF treatment in cells overexpressing either MEK1 or HRAS evoked significant levels of adipocytic differentiation. To ascertain that HRAS was promoting differentiation via the ERK pathway, we used the HRAS T35S mutant, which signals specifically through such an effector route (Rodriguez-Viciana et al., 1997). In agreement, this mutant also elicited significant levels of adipocytic differentiation upon EGF stimulation (Figure 8).

It was of interest to determine whether the nature of EGF signal could be altered by HRAS, depending on its sublocalization. To this end, we used the aforementioned site-specific HRAS constructs. Of interest, only overexpression of DM-tethered CD8-HRAS led to prolongation of ERK activation in response to EGF; overexpression of either GC KDELr-HRAS or ER-targeted PTP-HRAS was ineffective in this respect (Figure 7, A and B). In agreement, whereas overexpression of CD8-HRAS efficiently facilitated

FIGURE 4: Differential activation of RAS at different microdomains. (A) RAS distribution in plasma membrane and endomembranes of MCF-7 cells. Blots for transferrin receptor (Tfr) and calreticulin are used as respective markers. (B) Distribution of RAS isoforms in plasma membrane microdomains. Blots for Tfr (disordered membrane) and caveolin (lipid rafts) were used as microdomain markers. (C) RAS is not activated at ER. Cells transfected with HA-tagged PTP HRAS (0.5 µg), except (-), were left unstimulated (U) or treated with EGF (50 ng/ml) or HRG (30 ng/ml) for the indicated times. Cells transfected with RASGRF1 (1 µg) served as positive control. GTP loading was assayed by GST-RBD (RAF) pull down (PD). TL, total lysates. (D) RAS is not activated at GC. As in C, but cells were transfected with KDELr HRAS (0.5 µg). Cells transfected with RASGRP1 (1 µg) served as positive control. (E) RAS is activated in DM microdomains. As before, but in cells transfected with CD8 HRAS (0.5 µg).
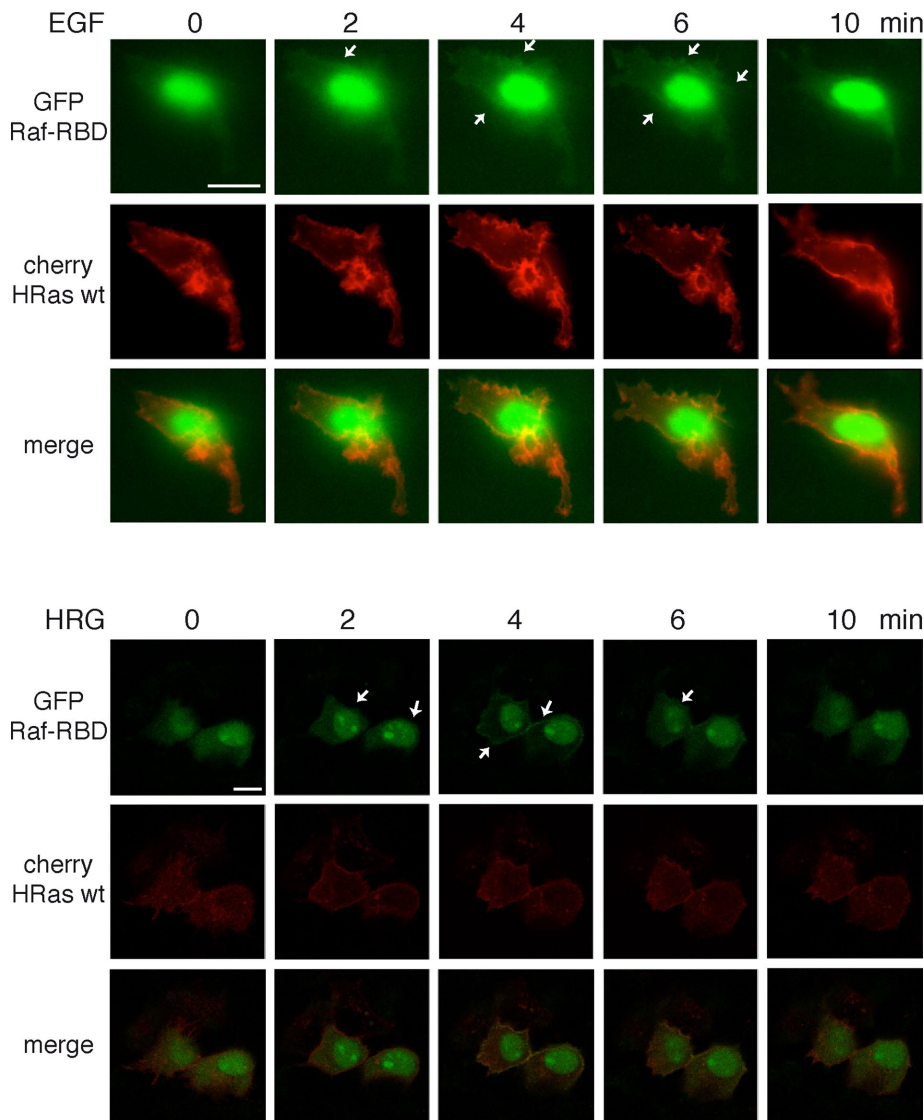
FIGURE 5: Live-cell imaging of RAS activation in response to EGF and HRG. MCF-7 cells were transfected with constructs expressing Cherry-HRAS and the RAS-GTP biosensor E3-R3(A/D) (1 μg each) and stimulated with (top) EGF (50 ng/ml) or (bottom) HRG (30 ng/ml) for the indicated times. Scale bars, 10 μm. Arrowheads show areas of prominent RAS-GTP accumulation.

the induction of adipocytic differentiation by EGF, this stimulus was incapable of evoking differentiation in cells harboring KDELr-HRAS or PTP-HRAS (Figure 7). These results demonstrate that HRAS is competent for prolonging EGF-induced ERK activation, and subsequently MCF-7 differentiation, only if its signals emanate from plasma membrane DM microdomains.

Nucleocytoplasmic ERK signal prolongation does not affect EGF output

We observed that stimulation with HRG resulted in sustained ERK phosphorylation at the nucleus and the cytoplasm, unlike EGF, which evoked transient activation at both compartments (Figure 3B). Thus we asked whether by prolonging ERK activation at either sublocalization we could transform the EGF signal into a differentiation stimulus. To this end, we transfected MCF-7 cells with MXI2, a p38 isoform that shuttles ERK to the nucleus (Casar et al., 2007), enhancing and prolonging ERK phosphorylation

there (Sanz-Moreno et al., 2003) by preventing its interaction with phosphatases (Casar et al., 2012). To sustain ERK signaling at the cytoplasm, we transfected cells with PEA15, a protein that serves as a cytoplasmic anchor for ERK, preventing its nuclear translocation (Formstecher et al., 2001). Because binding to PEA15 can affect ERK activity in some instances (Mace et al., 2013), we also prolonged ERK cytoplasmic activity by down-regulating the expression of the cytoplasmic phosphatase DUSP-6 using short hairpin RNAs (shRNAs; Caunt and Keyse, 2013). Indeed, the presence of MXI2 sustained EGF-induced ERK phosphorylation exclusively at the nucleus, whereas PEA15 overexpression or knockdown of DUSP-6 acted similarly at the cytoplasm (Figure 9A). However, none of these processes was capable of promoting adipocytic differentiation of MCF-7 cells in the presence of EGF (Figure 9B). These results demonstrated that prolonging ERK activation exclusively at the nucleus or at the cytoplasm is not sufficient to trigger differentiation in response to EGF stimulation.

Oncogenic HRAS induces apoptosis from different sublocalizations

The fact that neither proliferative nor differentiation stimuli induced RAS activation at endomembranes was intriguing, given that RAS seemed to be devoid of a biological function in these platforms. Of interest, expression of constitutively active, oncogenic RAS V12 in MCF-7 cells induced a potent apoptotic response (Figure 10A). Therefore we asked whether HRAS V12 could induce such an effect from endomembranes. To test this, we used the aforementioned sitespecific HRAS constructs, although in their oncogenic version, and tested their effects on MCF-7 viability by scoring growth of colonies in soft agar. HRAS V12 could evoke apoptosis from all of the sublocalizations tested, although with variable efficiency—the least intensively from ER and more pronouncedly from DM and the GC (Figure 10B)—thereby demonstrating that RAS at endomembranes was competent for conveying death signals.

RAS signals from the Golgi complex antagonize differentiation

The fact that ectopic HRAS V12 could trigger apoptogenic signaling from the GC indicated that some of the effector pathways used by RAS to convey signals downstream were functional at such sublocalization. Thus we asked whether activation of the endogenous isoform there could affect the differentiation response of MCF-7 cells. To activate the endogenous HRAS pool at the GC, we used overexpression of either RASGRP1, the guanosine nucleotide exchange factor (GEF) identified as responsible for RAS activation there (Bivona et al., 2003; Caloca et al., 2003), or of the RASGRF1 cdc25 domain specifically sent to the GC using the KDELr tethering cue
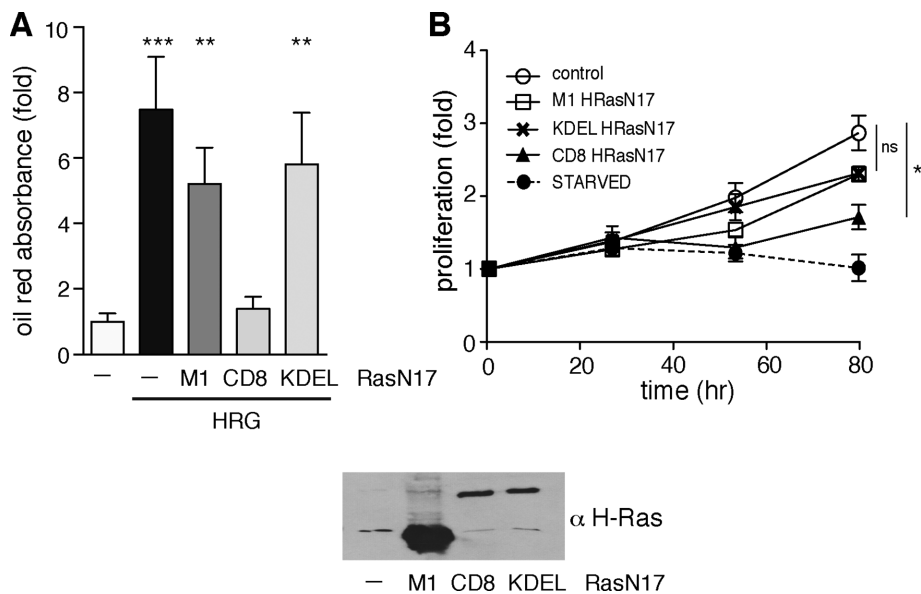
FIGURE 6: Effects of site-specific RAS blockade on differentiation and proliferation. (A) MCF-7 cells transfected with constructs expressing the indicated site-specific HRAS N17 mutants (1 µg) were stimulated with HRG (30 ng/ml) for 7 d before fixing and staining with Oil Red O. Bar chart shows the degree of differentiation quantified by extraction of the Oil Red O stain with isopropanol. Results show mean ± SEM of three independent experiments. **$p < 0.01$ and ***$p < 0.001$ with 95% confidence interval. Bottom, expression levels of the indicated HRAS N17 mutants. (B) The proliferation rate of cells expressing the indicated constructs was monitored over the indicated period of time. Results show mean ± SEM of three independent experiments. *$p < 0.05$; ns, not significant; 95% confidence interval.

(KDELr-Cdc25). HRG-induced adipocytic differentiation was significantly reduced in cells expressing either construct (Figure 10C). These results demonstrated that activation of the endogenous HRAS pool at the GC acted as a negative regulator of adipocytic differentiation and that within the same cellular context, RAS can exert different, even divergent, biological effects, depending on its sublocalization.

DISCUSSION

It is now established beyond doubt that the duration of RAS-ERK signals plays a critical role in the determination of cell fate in different types of cells (Traverse et al., 1992; McCawley et al., 1999; Liang and Chen, 2001; Nagashima et al., 2007). Similarly, the concept of space as a key factor in the regulation of Ras functions has been solidly supported by studies demonstrating that Ras proteins are present in different types of membranes (Choy et al., 1999; Chiu et al., 2002) and that within the PM, RAS isoforms occupy different microdomains (Prior et al., 2001). At these distinct sublocalizations, RAS is subject to site-specific regulation by different GEFs (Bivona et al., 2003; Caloca et al., 2003; Arozarena et al., 2004), engages different effector pathways (Matallanas et al., 2006), and switches on distinct genetic programs (Agudo-Ibanez et al., 2007). Here we studied how RAS-ERK signals integrate time and space in order to elicit a differentiation response. To do so, we used MCF-7 cells, in which transient ERK activation in response to EGF triggers proliferation, whereas prolonged ERK activation upon HRG treatment induces adipocytic differentiation, a process dependent on ERK activation, as our results using the MEK inhibitor U0126 demonstrate, in line with previous reports (Giani et al., 1998), although the participation of additional signaling pathways cannot be discarded.

Our results indicate that HRG evokes a sustained ERK signal. This is achieved at the level of ERK phosphorylation, since the activation

time course for other components of the pathway, such as RAS and MEK1, is much shorter. This rules out that HRG triggers some positive feedback mechanism, as described in other instances, such as for NGF-stimulated PC-12 cells (Santos et al., 2007). One possibility is that HRG down-regulates some phosphatase of the DUSP/MKP family or another type, thereby maintaining ERK in a phosphorylated state. In this respect, it has been shown that PP2A modulates HRG-induced ERK activation (Hatakeyama et al., 2003).

We observed that HRG evokes sustained ERK phosphorylation at both the cytoplasm and the nucleus. However, our data suggest that these two spatial components are not sufficient for inducing differentiation, as prolongation of ERK phosphorylation at the nucleus, as induced by MXI2, or at the cytoplasm, by PEA15 overexpression or DUSP-6 down-regulation, cannot elicit MCF-7 differentiation. One possibility is that our approaches for prolonging ERK activation, limited to the nucleus and the cytoplasm, do not fully recapitulate HRG effects, in the sense that activation of some other ERK spatial components, for example, at the mitochondria, might not be accomplished. A second possibility is that additional signals are requited for HRG-induced differentiation. In this respect, it was shown that HRG-evoked differentiation of MCF-7 cells requires PI-3K activation (Volinsky et al., 2015). Apparently, ERK can drive differentiation from either the nucleus or the cytoplasm, depending on the cell type. For example, cytoplasmic ERK promotes differentiation of endoderm (Smith et al., 2004) and muscle progenitor cells (Michailovici et al., 2014), whereas nuclear ERK activation drives neuronal differentiation in PC12 cells (Robinson et al., 1998). Thus it is likely that a correct combination of both the duration of ERK signal and its spatial specificity, referring to the precise cellular compartment(s) where it unfolds, is critical in the determination of cell fate.

RAS, due to its presence in multiple microenvironments, is a critical step for the acquisition of signal variability (Calvo et al., 2010; Ahearn et al., 2011; Arozarena et al., 2011), leading to different biological outputs. As expected, we showed that in MCF-7 cells, RAS is present both at the PM and in endomembranes like the ER and GC. At the PM, the presence of RAS is restricted to disordered membrane microdomains. Even the most abundant isoform, NRAS (Omerovic et al., 2008), is absent from cholesterol-rich domains. Although this might seem to be at odds with seminal findings allocating palmitoylated RAS in this type of membrane (Prior et al., 2001), we recently reported that RAS subject to palmitoylation displays a high, cell type–dependent variability in its distribution at different PM microdomains (Agudo-Ibanez et al., 2015). Of interest, RAS mediates both proliferative (EGF) and differentiation (HRG) stimuli exclusively from the PM, not from endomembranes. This is not unprecedented with respect to EGF, as previous reports in different cell types demonstrated that it activates RAS solely at the cell periphery (Augsten et al., 2006; Song et al., 2013; Pinilla-Macua et al., 2016). We showed that RAS, when present at disordered membrane microdomains, can also induce apoptosis if it is constitutively active. The
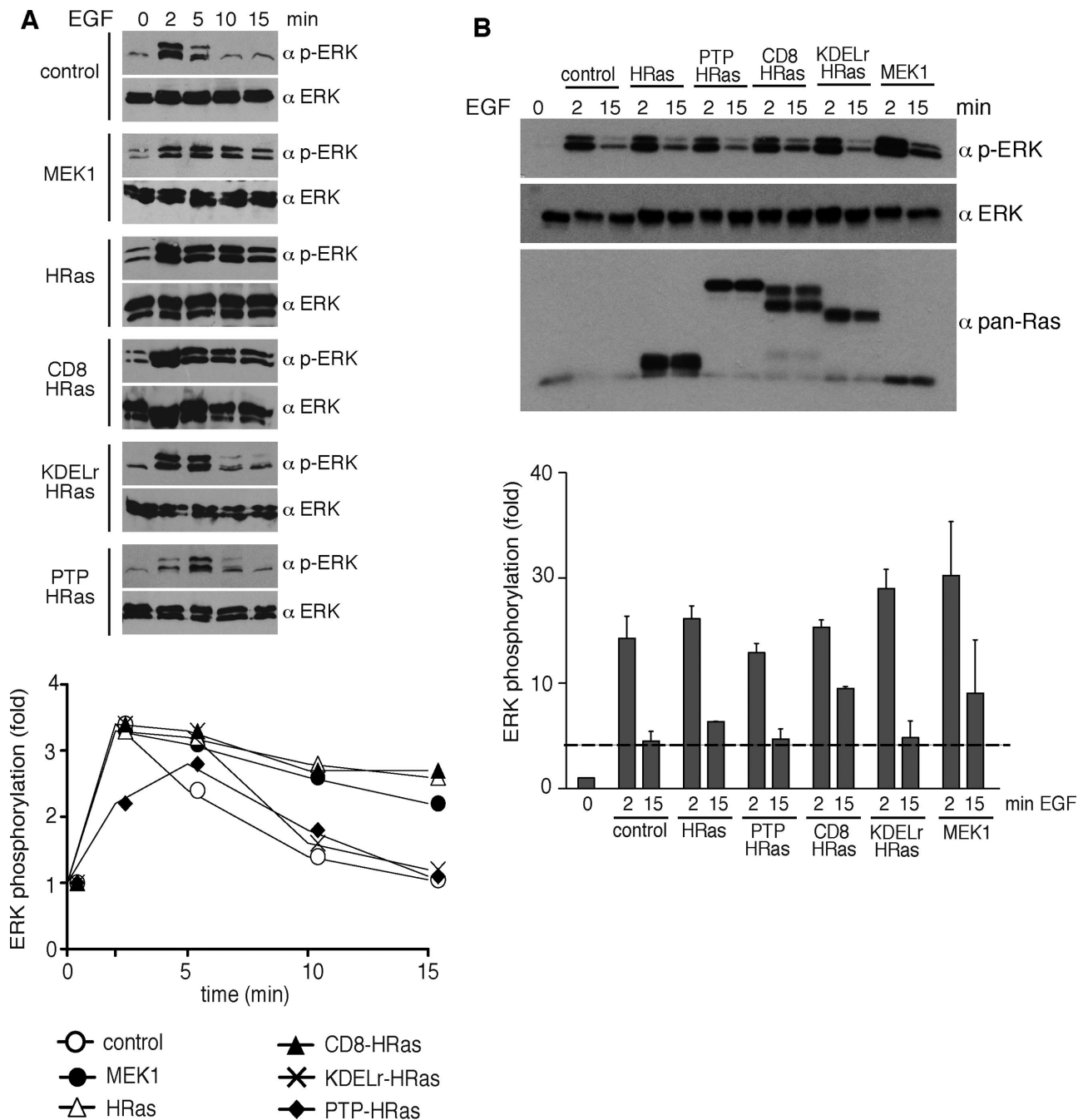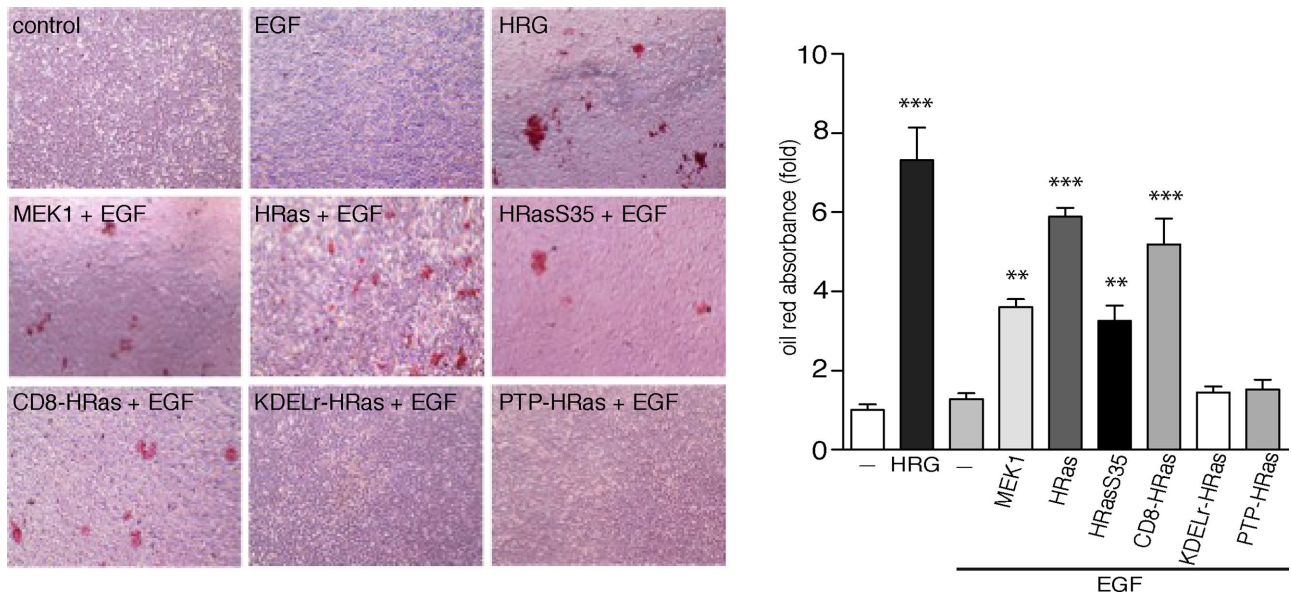
FIGURE 7: Overexpression of upstream components of the RAS-ERK pathway prolongs ERK phosphorylation. (A) MCF-7 cells transfected with constructs expressing the indicated proteins (5 µg) were stimulated with EGF (50 ng/ml) for the indicated times, and ERK phosphorylation was assayed by immunoblotting. Graph shows results mean from three independent experiments. (B) For comparative purposes, ERK phosphorylation levels after 2 and 15 min of EGF stimulation from cells expressing the indicated proteins were evaluated in the same gel. Graph quantitates mean ± SEM of three independent experiments relative to the levels in unstimulated cells (0).

fact that oncogenic RAS induces a potent apoptotic response in MCF-7 cells could help to explain why RAS mutations are so rare in mammary tumors.

Thus our results suggest that because signals evoking different, even antagonistic, outcomes can originate from the same sublocalization, in the case of mammary epithelial cells, the determination of cell fate by RAS-ERK signals would be primarily dictated, not by spatial considerations, but by the duration of the RAS signal: a transient

signal evokes proliferation, a prolonged one leads to differentiation, and a constant signal causes cell death. However, we found that apoptosis can also be potently induced by oncogenic RAS from endomembranes like the GC. Along this line, a recent study showed that oncolytic viruses induce apoptosis by promoting RAS signals at such compartments (Garant et al., 2016). The RAS proapoptotic effect at the GC could explain why proliferative and differentiation stimuli, like those evoked by EGF and HRG, respectively, avoid

FIGURE 8: Overexpression of upstream components of the RAS-ERK pathway facilitates EGF-induced differentiation. MCF-7 cells transfected with constructs expressing the indicated proteins (5 µg) were stimulated with EGF (50 ng/ml) or HRG (30 ng/ml) for 7 d before fixing and staining with Oil Red O. Bar chart shows the degree of differentiation quantified by extraction of the Oil Red O stain with isopropanol. Results show mean ± SEM of three independent experiments. **$p < 0.01$ and ***$p < 0.001$ with 95% confidence interval.

activating this RAS pool. In agreement, we showed that activation of endogenous RAS at the GC antagonizes differentiation as induced by HRG. Overall our results indicate that distinct spatiotemporally defined RAS signals can mediate antagonistic biological outputs. Thus, ultimately, cell destiny would be defined by the ability of a stimulus to activate RAS at the appropriate sublocalization for the adequate period of time while avoiding switching on opposing RAS signals.

MATERIALS AND METHODS
Plasmids
Plasmids encoding HRAS wild type (wt), HRAS V12, and Lck-, M1-, KDELr-, CD8-tethered HRAS wild-type and N17 versions (Matallanas *et al.*, 2006), MEK1 wt and Ha-MXI2 (Casar *et al.*, 2007), and RASGRP1 (Arozarena *et al.*, 2004) have been described previously. PTP-tethered HRAS (Lorentzen *et al.*, 2010) was provided by P. Bastiaens (MPI, Dortmund). HRAS S35 was provided by J. Downward (Francis Crick Institute, London). KDELr-CDC25 was constructed following a strategy previously described (Matallanas *et al.*, 2006) by fusing RasGRF1 Cdc25 domain C-terminal to KDELr N193D. shRNAs against DUSP6 were from Dharmacon.

Cell culture
MCF-7 cells were grown in DMEM supplemented with 10% fetal calf serum. Cells were transfected with Lipofectamine (Invitrogen, Waltham, MA) following the manufacturer's instructions. Stable cell lines were selected with 750 mg/ml G418 or 300 µg/ml Zeocin (Invitrogen). EGF, HRG, and U0126 were from Calbiochem, San Diego, CA. Adipocytic staining with Oil Red O and quantification by extraction with isopropanol were performed as described previously (Peregrin *et al.*, 2006). Cell proliferation was analyzed basically as described (Rodriguez *et al.*, 2010).

Antibodies
Mouse monoclonal anti-hemagglutinin (HA) and rabbit polyclonals anti-RhoGDI, anti-HRAS, anti-panRAS, anti-PEA15, anti-RSK1 anti–p-ERK,

and anti-ERK2 were from Santa Cruz Biotechnology, Santa Cruz, CA. Rabbit polyclonal anti-p-RSK-1, anti-ELK1, and anti-p-ELK1 were from Cell Signaling, Billerica, MA. Rabbit polyclonal anti-caveolin and anti–lamin A were from BD Biosciences, San Jose, CA. Mouse monoclonal anti–transferrin receptor was from Zymed Laboratories, Waltham, MA. Rabbit polyclonal anti-calreticulin was from Calbiochem.

Immunoblotting
Samples were fractionated by SDS–PAGE and transferred onto nitrocellulose filters as described previously (Ajenjo *et al.*, 2000). Immunocomplexes were visualized by enhanced chemiluminescence detection (GE Healthcare, Little Chalfont, United Kingdom) by using horseradish peroxidase–conjugated secondary antibodies (Bio-Rad Laboratories, Hercules, CA).

Time-lapse immunofluorescence
Cells were grown on polylysine-coated, glass-bottom dishes and transiently cotransfected with Cherry-HRAS wt and GFP-RAF RBD E3-R3(A/D) (Augsten *et al.*, 2006). Cells were deprived of serum, placed into a microscope chamber, and treated with EGF or HRG. Confocal images (512 × 512 pixels; 0.15-pixel size) were acquired at 37°C in a TCS SP-5 confocal microscope (Leica, Wetzlar, Germany) with a 40×, 1.25 numerical aperture numerical aperture oil objective, a 1-Airy pinhole, and 200-Hz speed. Images were captured every 2 min for a period of at least 1 h after stimulation. Cells were excited with 458- and 543-nm laser lines. Images presented are after digital adjustment of brightness and contrast to maximize signal.
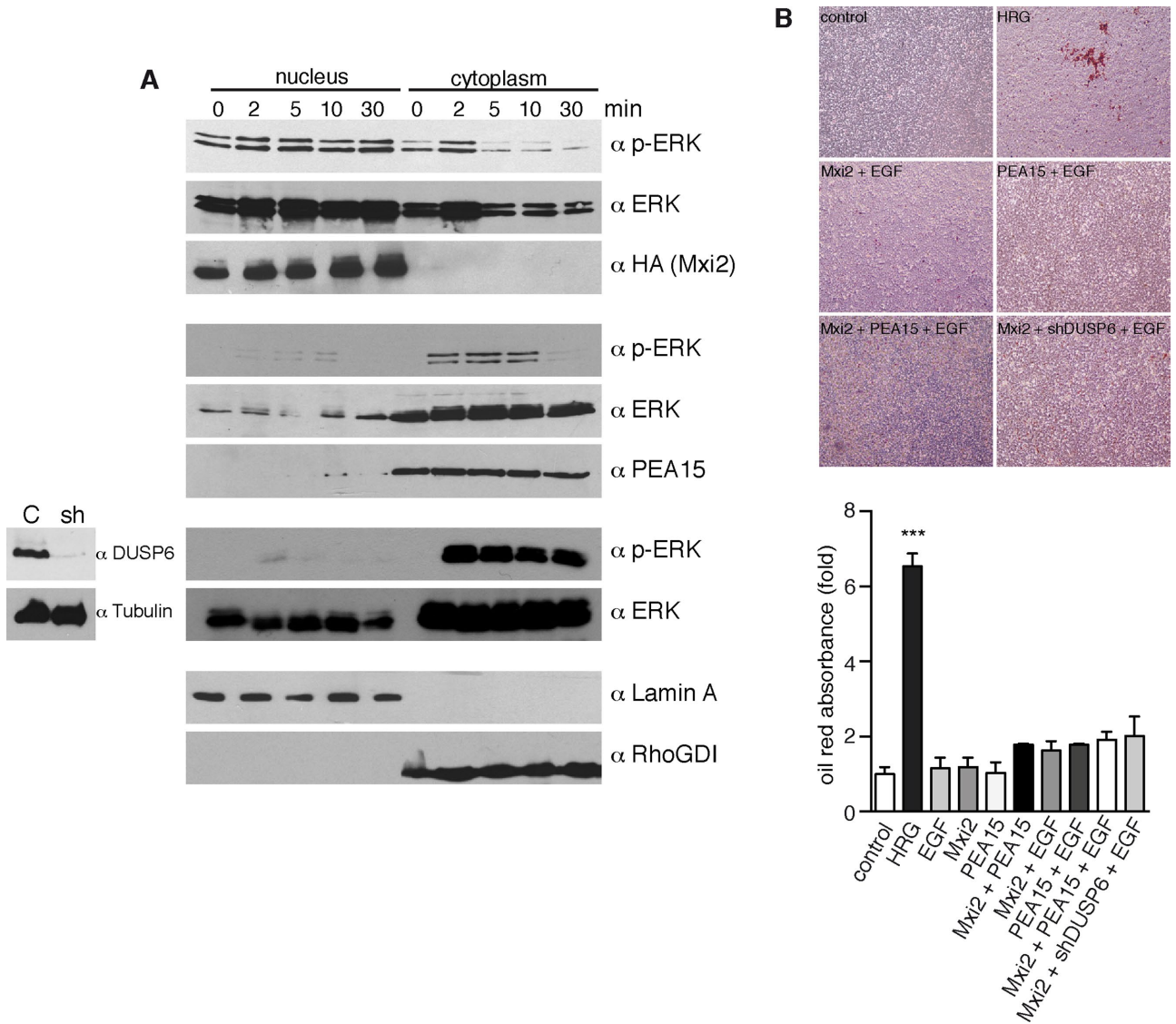
Nucleocytoplasmic fractionations
Nucleocytoplasmic fractionations were performed exactly as described (Sanz-Moreno *et al.*, 2003).

Plasma membrane fractionation in sucrose gradients
Cells were collected and treated as described previously (Matallanas *et al.*, 2006). Briefly, cells were resuspended in 25 mM

FIGURE 9: Effects of sustaining ERK phosphorylation at the cytoplasm and nucleus on differentiation. (A) Time course of ERK phosphorylation in nuclear and cytoplasmic fractions of cells transfected with MXI2, PEA15 (1 μg), or shRNAs against DUSP6 and treated with EGF (50 ng/ml) for the indicated times. The purity of the fractions was ascertained by immunoblotting with lamin A and RhoGDI as nuclear and cytoplasmic markers, respectively. Left, evaluation of DUSP-6 down-regulation by shRNAs (sh). (B) Effects of the indicated constructs plus EGF treatment on differentiation. Bar chart shows the degree of differentiation quantified by extraction of the Oil Red O stain with isopropanol. Results show mean ± SEM of three independent experiments. ***$p < 0.001$ with 95% confidence interval.

Tris, pH 7.4, 150 mM NaCl, 5 mM EDTA, and 0.25% Triton X-100 plus protease inhibitor cocktail (1 μg/ ml). Lysates were set at a sucrose concentration of 45%. Layers of 3.4 ml of 35% sucrose and 1 ml of 16% sucrose were sequentially overlaid and centrifuged for 18 h at 41,000 rpm (MLS-50 rotor; Beckman, San Diego, CA). Twelve 0.4-ml fractions were collected and resuspended directly into SDS–PAGE sample buffer for analysis by immunoblotting.

Plasma membrane–endomembrane fractionation in sucrose gradients

Cells from four 100-mm plates were collected and lysed in hypotonic buffer (10 mM 4-(2-hydroxyethyl)-1-piperazineethanesulfonic acid, pH 7.3, 1.5 mM MgCl$_2$, and 5 mM KCl plus protease inhibitor cocktail, 1 μg/ ml). Lysates were homogenized by passage through a 5-μm/8.0-mm douncer and centrifuged (700 × g for 3 min at 4°C).

The supernatant was subjected to a new centrifugation (40,000 × g for 30 min at 4°C). The pellet containing the membranes was resuspended in homogenizing buffer (20 mM Tris, pH 7.4, 5 mM MgCl$_2$, 25 mM KCl, 0.25% sucrose) and laid onto a discontinuous layer of iodixanol 2.5–30% to be centrifuged at 100,000 × g for 5–6 h at 4°C.

Ras-GTP loading assays

Ras-GTP loading assays were performed as described previously (Arozarena et al., 2000). H-Ras-GTP was affinity sequestered by using glutathione S-transferase (GST)–RAF-RBD. Immunoblots were performed with anti-HA antibody and quantified by densitometry using ImageJ (National Institutes of Health, Bethesda, MD). Activation levels were related to total protein levels as determined by anti-HA immunoblotting in the corresponding total lysates.
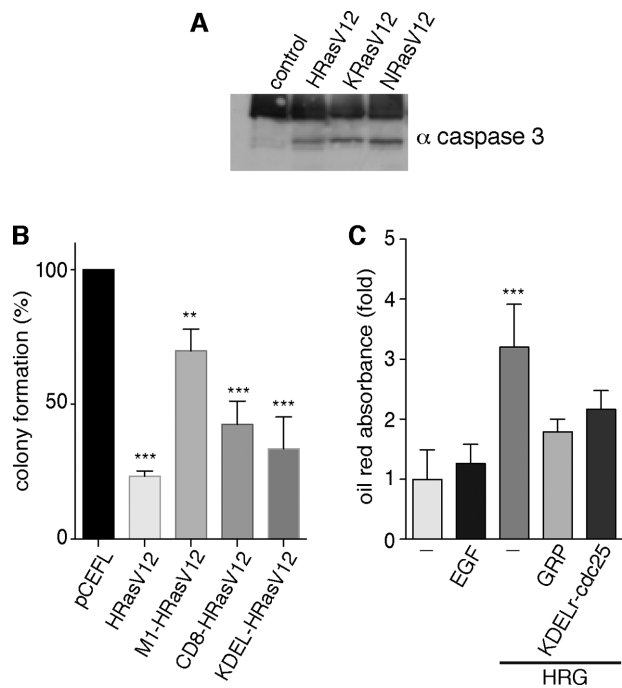
FIGURE 10: Oncogenic HRAS induces apoptosis in MCF-7 cells. (A) Induction of apoptosis in cells transfected with RAS V12 oncogenic isoforms (1 µg), as evaluated by assaying for cleaved caspase 3. (B) Effects of the indicated site-specific HRAS V12 constructs (1 µg) on cell viability, scored in soft agar colonies. (C) Activation of endogenous RAS at the GC prevents HRG-induced differentiation. Cells transfected with RASGRP1 or KDEL-cdc25 (1 µg) were treated with HRG (30 ng/ml) for 7 f before fixing and staining with Oil Red. **$p < 0.01$, ***$p < 0.001$ with 95% confidence interval.

Statistical analyses

All statistical data were analyzed and compared for statistically significant differences by Student's *t* test (GraphPad Software, San Diego, CA).

REFERENCES

Agudo-Ibanez L, Herrero A, Barbacid M, Crespo P (2015). H-ras distribution and signaling in plasma membrane microdomains are regulated by acylation and deacylation events. Mol Cell Biol 35, 1898–1914.

Agudo-Ibanez L, Nunez F, Calvo F, Berenjeno IM, Bustelo XR, Crespo P (2007). Transcriptomal profiling of site-specific Ras signals. Cell Signal 19, 2264–2276.

Ahearn IM, Haigis K, Bar-Sagi D, Philips MR (2011). Regulating the regulator: post-translational modification of RAS. Nat Rev Mol Cell Biol 13, 39–51.

Ajenjo N, Aaronson DS, Ceballos E, Richard C, León J, Crespo P (2000). Myeloid leukemia cell growth and differentiation are independent of mitogen-activated protein kinases ERK1/2 activation. J Biol Chem 275, 7189–7197.

Albeck JG, Mills GB, Brugge JS (2013). Frequency-modulated pulses of ERK activity transmit quantitative proliferation signals. Mol Cell 49, 249–261.

Arozarena I, Aaronson DS, Matallanas D, Sanz V, Ajenjo N, Tenbaum SP, Teramoto H, Ighishi T, Zabala JC, Gutkind JS, et al. (2000). The Rho family GTPase Cdc42 regulates the activation of Ras/MAP kinase by the exchange factor Ras-GRF. J Biol Chem 275, 26441–26448.

Arozarena I, Calvo F, Crespo P (2011). Ras, an actor on many stages: post-translational modifications, localization, and site-specified events. Genes Cancer 2, 182–194.

Arozarena I, Matallanas D, Berciano MT, Sanz-Moreno V, Calvo F, Munoz MT, Egea G, Lafarga M, Crespo P (2004). Activation of H-Ras in the endoplasmic reticulum by the RasGRF family guanine nucleotide exchange factors. Mol Cell Biol 24, 1516–1530.

Augsten M, Pusch R, Biskup C, Rennert K, Wittig U, Beyer K, Blume A, Wetzker R, Friedrich K, Rubio I (2006). Live-cell imaging of endogenous Ras-GTP illustrates predominant Ras activation at the plasma membrane. EMBO Rep 7, 46–51.

Bivona TG, Perez de Castro I, Ahearn IM, Grana TM, Chiu VK, Lockyer PJ, Cullen PJ, Pellicer A, Cox AD, Philips MR (2003). Phospholipase Cg activates Ras on the Golgi apparatus by means of RasGRP1. Nature 424, 694–698.

Caloca MJ, Zugaza JL, Bustelo XR (2003). Exchange factors of the RasGRP family mediate Ras activation in the Golgi. J Biol Chem 278, 33465–33473.

Calvo F, Agudo-Ibanez L, Crespo P (2010). The Ras-ERK pathway: understanding site-specific signaling provides hope of new anti-tumor therapies. Bioessays 32, 412–421.

Casar B, Rodriguez J, Gibor G, Seger R, Crespo P (2012). Mxi2 sustains ERK1/2 phosphorylation in the nucleus by preventing ERK1/2 binding to phosphatases. Biochem J 441, 571–578.

Casar B, Sanz-Moreno V, Yazicioglu MN, Rodriguez J, Berciano MT, Lafarga M, Cobb MH, Crespo P (2007). Mxi2 promotes stimulus-independent ERK nuclear translocation. EMBO J 26, 635–646.

Caunt CJ, Keyse SM (2013). Dual-specificity MAP kinase phosphatases (MKPs): shaping the outcome of MAP kinase signalling. FEBS J 280, 489–504.

Chiu VK, Bivona T, Hach A, Sajous JB, Silletti J, Wiener H, Johnson RL, Cox AD, Philips MR (2002). Ras signaling on the endoplasmic reticulum and the golgi. Nat Cell Biol 4, 343–350.

Choy E, Chiu VK, Silletti J, Feoktistov M, Morimoto T, Michaelson D, Ivanov IE, Philips MR (1999). Endomembrane trafficking of Ras: the CAAX motif targets proteins to the ER and Golgi. Cell 98, 69–80.

Formstecher E, Ramos JW, Fauquet M, Calderwood DA, Hsieh JC, Canton B, Nguyen XT, Barnier JV, Camonis J, Ginsberg MH, et al. (2001). PEA-15 mediates cytoplasmic sequestration of ERK MAP kinase. Dev Cell 1, 239–250.

Garant KA, Shmulevitz M, Pan L, Daigle RM, Ahn DG, Gujar SA, Lee PW (2016). Oncolytic reovirus induces intracellular redistribution of Ras to promote apoptosis and progeny virus release. Oncogene 35, 771–782.

Giani C, Casalini P, Pupa SM, De Vecchi R, Ardini E, Colnaghi MI, Giordano A, Menard S (1998). Increased expression of c-erbB-2 in hormone-dependent breast cancer cells inhibits cell growth and induces differentiation. Oncogene 17, 425–432.

Hatakeyama M, Kimura S, Naka T, Kawasaki T, Yumoto N, Ichikawa M, Kim JH, Saito K, Saeki M, Shirouzu M, et al. (2003). A computational model on the modulation of mitogen-activated protein kinase (MAPK) and Akt pathways in heregulin-induced ErbB signalling. Biochem J 373, 451–463.

Kholodenko BN, Hancock JF, Kolch W (2010). Signalling ballet in space and time. Nat Rev Mol Cell Biol 11, 414–426.

Liang CC, Chen HC (2001). Sustained activation of extracellular signal-regulated kinase stimulated by hepatocyte growth factor leads to integrin alpha 2 expression that is involved in cell scattering. J Biol Chem 276, 21146–21152.

Lorentzen A, Kinkhabwala A, Rocks O, Vartak N, Bastiaens PI (2010). Regulation of Ras localization by acylation enables a mode of intracellular signal propagation. Sci Signal 3, ra68.

Mace PD, Wallez Y, Egger MF, Dobaczewska MK, Robinson H, Pasquale EB, Riedl SJ (2013). Structure of ERK2 bound to PEA-15 reveals a mechanism for rapid release of activated MAPK. Nat Commun 4, 1681.

Matallanas D, Sanz-Moreno V, Arozarena I, Calvo F, Agudo-Ibanez L, Santos E, Berciano MT, Crespo P (2006). Distinct utilization of effectors and biological outcomes resulting from site-specific Ras activation: Ras functions in lipid rafts and Golgi complex are dispensable for proliferation and transformation. Mol Cell Biol 26, 100–116.

McCawley LJ, Li S, Wattenberg EV, Hudson LG (1999). Sustained activation of the mitogen-activated protein kinase pathway. A mechanism underlying receptor tyrosine kinase specificity for matrix metalloproteinase-9 induction and cell migration. J Biol Chem 274, 4347–4353.

Michailovici I, Harrington HA, Azogui HH, Yahalom-Ronen Y, Plotnikov A, Ching S, Stumpf MP, Klein OD, Seger R, Tzahor E (2014). Nuclear to cytoplasmic shuttling of ERK promotes differentiation of muscle stem/progenitor cells. Development 141, 2611–2620.

Nagashima T, Shimodaira H, Ide K, Nakakuki T, Tani Y, Takahashi K, Yumoto N, Hatakeyama M (2007). Quantitative transcriptional control of ErbB receptor signaling undergoes graded to biphasic response for cell differentiation. J Biol Chem 282, 4045–4056.

Omerovic J, Hammond DE, Clague MJ, Prior IA (2008). Ras isoform abundance and signalling in human cancer cell lines. Oncogene 27, 2754–2762.

Peregrin S, Jurado-Pueyo M, Campos PM, Sanz-Moreno V, Ruiz-Gomez A, Crespo P, Mayor F Jr, Murga C (2006). Phosphorylation of p38 by GRK2 at the docking groove unveils a novel mechanism for inactivating p38MAPK. Curr Biol 16, 2042–2047.

Pinilla-Macua I, Watkins SC, Sorkin A (2016). Endocytosis separates EGF receptors from endogenous fluorescently labeled HRas and diminishes receptor signaling to MAP kinases in endosomes. Proc Natl Acad Sci USA 113, 2122–2127.

Prior IA, Harding A, Yan J, Sluimer J, Parton RG, Hancock JF (2001). GTP-dependent segregation of H-ras from lipid rafts is required for biological activity. Nat Cell Biol 3, 368–375.

Robinson MJ, Stippec SA, Goldsmith E, White MA, Cobb MH (1998). A constitutively active and nuclear form of MAP kinase ERK2 is sufficient for neurite outgrowth and cell transformation. Curr Biol 8, 1141–1150.

Rodriguez J, Calvo F, Gonzalez JM, Casar B, Andres V, Crespo P (2010). ERK1/2 MAP kinases promote cell cycle entry by rapid, kinase-independent disruption of retinoblastoma-lamin A complexes. J Cell Biol 191, 967–979.

Rodriguez-Viciana P, Warne PH, Khwaja A, Marte BM, Pappin D, Das P, Waterfield MD, Ridley A, Downward J (1997). Role of phosphoinositide 3-OH kinase in cell transformation and control of the actin cytoskeleton by Ras. Cell 89, 457–467.

Santos SD, Verveer PJ, Bastiaens PI (2007). Growth factor-induced MAPK network topology shapes Erk response determining PC-12 cell fate. Nat Cell Biol 9, 324–330.

Sanz-Moreno V, Casar B, Crespo P (2003). p38alpha isoform Mxi2 binds to extracellular signal-regulated kinase 1 and 2 mitogen-activated protein kinase and regulates its nuclear activity by sustaining its phosphorylation levels. Mol Cell Biol 23, 3079–3090.

Smith ER, Smedberg JL, Rula ME, Xu XX (2004). Regulation of Ras-MAPK pathway mitogenic activity by restricting nuclear entry of activated MAPK in endoderm differentiation of embryonic carcinoma and stem cells. J Cell Biol 164, 689–699.

Song SP, Hennig A, Schubert K, Markwart R, Schmidt P, Prior IA, Bohmer FD, Rubio I (2013). Ras palmitoylation is necessary for N-Ras activation and signal propagation in growth factor signalling. Biochem J 454, 323–332.

Traverse SN, Gomez N, Paterson H, Marshall CJ, Cohen P (1992). Sustained activation of the mitogen-activated protein (MAP) kinase cascade may be required for differentiation of PC12 cells. Biochem J 288, 351–355.

Volinsky N, McCarthy CJ, von Kriegsheim A, Saban N, Okada-Hatakeyama M, Kolch W, Kholodenko BN (2015). Signalling mechanisms regulating phenotypic changes in breast cancer cells. Biosci Rep 35, e00178.